PERGAMON

European Polymer Journal 35 (1999) 1393–1401

EUROPEAN POLYMER JOURNAL

Kinetics of quenching of polymer-bound ruthenium (II) complexes with MV^{2+} containing L-tyrosine esters

M. Suzuki, M. Sano, M. Kimura, K. Hanabusa, H. Shirai *

Department of Functional Polymer Science, Faculty of Textile Science and Technology, Shinshu University, Ueda, Nagano 386-8567, Japan

Received 10 July 1998; accepted 3 September 1998

Abstract

The effects of L-tyrosine esters with hexyl (C_6Tyr), octyl (C_8Tyr) and dodecyl (C_{12}Tyr) groups on quenching of partially quaternized poly(1-vinylimidazole)-bound ruthenium (II) complexes (RuQPIm-19 and RuQPIm-44, the numbers represent the degree of quaternization in molar percentage) with the 1,1′-dimethyl-4,4′-bipyridinium dication (methylviologen: MV^{2+}) have been kinetically investigated in methanol. In the absence of L-tyrosine esters, the Stern–Volmer plots for RuQPIm-19 and RuQPIm-44 showed an upward deviating curve and a straight line, respectively. This result indicated that the quenching mechanism depended significantly on the degree of quaternization. The computed curve fitting to the observed Stern–Volmer plots showed that the quenching reaction proceeded through only a static quenching process for RuQPIm-19 and through only a dynamic quenching process for RuQPIm-44. In the presence of L-tyrosine esters, the Stern–Volmer plots for quenching of RuQPIm-44 showed downward deviating curves, indicating that these quenching reactions proceeded through both dynamic quenching and static quenching processes. This was supported by the fact that the curve fitting according to the theoretical equation reported as a combination of dynamic and static quenching models agreed well with the observed Stern–Volmer plots. On the other hand, although the quenching reactions for RuQPIm-19 systems also proceeded through mediated and non-mediated processes, both were static quenching processes; namely, the quenching reactions proceeded through two different static quenching mechanisms. A new Stern–Volmer plot for the systems was proposed and the kinetic parameters were estimated. Furthermore, it was found that the quenching rate constants for the mediated processes were faster than those for the dynamic quenching process in the RuQPIm-44 and the statically non-mediated process in the RuQPIm-19.

1. Introduction

In biological systems, many redox proteins undergo long-range electron transfer involving electron tunneling through polypeptides, and their kinetics and reaction mechanisms have been extensively studied [1–3]. Such investigations using modified proteins [4, 5] have suggested that some amino acid residues in the proteins would participate in the long-range electron transfer in biological systems [6–8]. For example, photoinduced electron transfer in the photosynthesis of green plants occurs through tyrosine residues [9]. In these electron transfer systems, however, modified enzyme systems and synthetic donor–acceptor systems, which are difficult to modify, synthesize and characterize, have been mainly employed. For simple systems, the electron transfer reaction in a natural polymer matrix has been reported [10], and some polymer systems containing donors and acceptors have also been studied [11, 12]. The pathway effect in photoinduced electron transfer from $Ru(bpy)_3^{2+}$ (bpy = 2,2′-bipyridine) to methylviologen in a synthetic polymer film has been investigated, and the electron transfer distance was found to double in the presence of 3-methylindole

* Corresponding author. Fax: +81-268-24-7248; e-mail: smasa@giptc.shinshu-u.ac.jp

0014-3057/99/$ - see front matter
PII: S0014-3057(98)00224-9

as a tryptophan residue model [13]. Further, for electrochemical water oxidation in a polymer membrane, the charge transfer distance is increased by the addition of *p*-cresol from 1.28 to 2.25 nm, showing that *p*-cresol functions as a mediator for the charge transport [14].

Recently, partially quaternized poly(1-vinylimidazole)-bound ruthenium (II) complexes (RuQPIm) as polymer photosensitizers have been employed for photosensitized charge separation and photoinduced hydrogen generation reactions [15–17]. In the quenching reaction of RuQPIms with methylviologen, the quenching efficiency depended significantly on the degree of quaternization; it decreased with increasing degree of quaternization [18]. Furthermore, a Stern–Volmer plot showed an upward deviating curve at a low degree of quaternization, while it showed a straight line at a high degree of quaternization. These results led us to conclude that the quenching mechanism changed with the degree of quaternization. In the present paper, we report the kinetics and mechanism of quenching of RuQPIms with methylviologen and the effect of L-tyrosine esters.

2. Experimental

2.1. Materials

L-Tyrosine, alkyl alcohols, and other synthesis reagents (commercially available guaranteed reagents) were used without further purification. 1,1′-Dimethyl-4,4′-bipyridinium chloride (methylviologen; MV^{2+}) was purchased from TCI Co. Ltd, and recrystallized from methanol. Polymer-bound ruthenium (II) complexes (RuQPIm-19 and RuQPIm-44: the numbers represent the molar percentage of quaternized imidazolium residues) were prepared according to a method described elsewhere [15, 19]. *cis*-Bis(2,2′-bipyridine)di(1-methylimidazole)ruthenium (II) hexafluorophosphate $\{[Ru(bpy)_2(MeIm)_2](PF_6)_2\}$ as a low molecular weight model complex was prepared by refluxing a methanol solution of *cis*-bis(2,2′-bipyridine)dichlororuthenium (II) and 1-methylimidazole for three days under an argon atmosphere. The ruthenium (II) complex was characterized using UV–vis absorption, luminescence, Fourier-transform infrared (FTIR) and ^{1}H-NMR spectroscopies and elemental analysis. L-tyrosine esters with hexyl (C_6Tyr), octyl (C_8Tyr) and dodecyl (C_{12}Tyr) groups were prepared by a modified version of the thionyl chloride method [20] Fig. 1. To an alkyl alcohol at 0°C, thionyl chloride (55 mmol) and then L-tyrosine (5 mmol) were added. The resulting suspension was stirred at 70°C for 12 h. After cooling to room temperature, 300 ml of ethyl ether was added. The white precipitate was collected by filtration, sufficiently

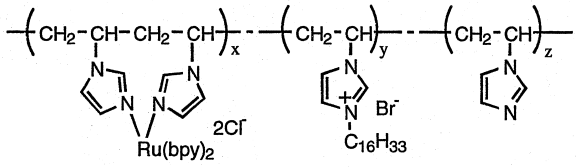

Polymers	x	y	z
RuQPIm-19	0.0035	0.1915	0.8050
RuQPIm-44	0.0035	0.4404	0.5561

Fig. 1. Chemical structure of RuQPIm.

washed with ethyl ether, and dried. These L-tyrosine esters were purified by recrystallization from methanol-ethyl ether. Identification was carried out by ^{1}H-NMR spectroscopy and elemental analysis.

2.2. Measurements

UV–vis spectra were recorded on a JASCO V-570 UV/VIS/NIR spectrophotometer. Luminescence spectra were recorded on a Hitachi 650-10 S fluorescence spectrophotometer. Luminescence lifetimes for these ruthenium (II) complexes were measured using a Horiba NASE-550 nanosecond fluorometer.

The quenching reaction was carried out at 25°C under an argon atmosphere in methanol. Sample solutions were adjusted to $[Ru(II)] = 2.0 \times 10^{-5}$ mol dm^{-3}, [L-tyrosine esters] = 5.0×10^{-2} mol dm^{-3}, and [Viologen] = 0–5.0×10^{-3} mol dm^{-3}. The luminescence at 648 nm from the triplet metal-to-ligand charge-transfer (MLCT) state [15, 21], which was excited at 488 nm, was monitored as a function of the concentration of viologen.

3. Results

The luminescence quenching of 2.0×10^{-5} mol dm^{-3} RuQPIm-44 in methanol at 25°C using MV^{2+} is shown in Fig. 2. A change in the luminescence spectral profile was not observed, indicating the absence of an emitting excited state complex under these experimental conditions.

3.1. Absence of L-tyrosine esters

Fig. 3 shows Stern–Volmer plots for the quenching of RuQPIm-19, RuQPIm-44 and $Ru(bpy)_2(MeIm)_2^{2+}$ with MV^{2+} in methanol. The Stern–Volmer plot for RuQPIm-19 showed an upward deviating curve, while it showed straight lines for RuQPIm-44 and $Ru(bpy)_2(MeIm)_2^{2+}$. These results indicate that the quenching reaction

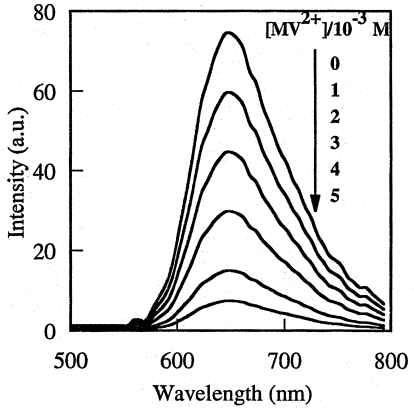

Fig. 2. Luminescence spectral changes of RuQPIm-44 with increasing concentration of MV^{2+} in methanol.

proceeds through a dynamic process for RuQPIm-44 and $Ru(bpy)_2(MeIm)_2^{2+}$ and through both dynamic and static processes or only a static process for RuQPIm-19.

For RuQPIm-44 and $Ru(bpy)_2(MeIm)_2^{2+}$ systems, the quenching reaction proceeds through a dynamic process due to the linear Stern–Volmer plot and no interaction of the MV^{2+} species of the ruthenium (II) complex residue, and can be expressed by Eqs. (1)–(4):

$$Ru \xrightarrow{h\nu'} {}^*Ru \tag{1}$$

$${}^*Ru \xrightarrow{k_e} Ru + h\nu \tag{2}$$

$${}^*Ru \xrightarrow{k_d} Ru \tag{3}$$

$${}^*Ru \xrightarrow{kq_2[MV^{2+}]} Ru \tag{4}$$

where kq_2 is a second-order quenching constant, and

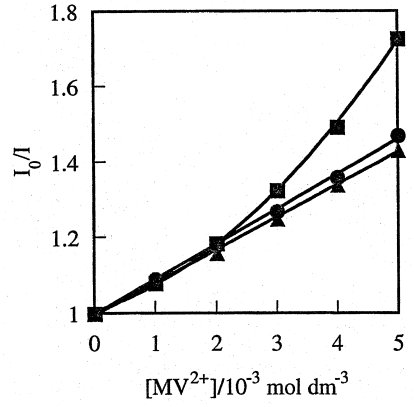

Fig. 3. Stern–Volmer plots for quenching of ruthenium (II) complexes with MV^{2+} for RuQPIm-19 (■), RuQPIm-44 (▲) and $Ru(bpy)_2(MeIm)_2^{2+}$ (●).

k_d and k_e are the rate constants of the nonluminescent and luminescent decays of the photoexcited ruthenium (II) complex. The Stern–Volmer plot for the dynamic quenching process can be expressed by Eq. (5) [22]:

$$I_0/I = 1 + Ksv[MV^{2+}], \quad Ksv = kq_2 \times \tau_0 \tag{5}$$

where Ksv is a Stern–Volmer constant which is given by the product of the second-order quenching rate constant kq_2 and the lifetime of the probe in the absence of quencher τ_0. According to Eq. (5), the Stern–Volmer plot for the dynamic quenching process gives a straight line. For RuQPIm-44 and $Ru(bpy)_2(MeIm)_2^{2+}$, as predicted by Eq. (1), these plots are linear ($R^2 = 0.999$). Therefore, the quenching reactions for these systems take place only through a dynamic quenching process. The values of Ksv, τ_0 and kq_2 are summarized in Table 1. Compared with the $Ru(bpy)_2(MeIm)_2^{2+}$ system, the quenching constant for the RuQPIm-44 system is small because the RuQPIm-44 has many positively charged groups around the ruthenium (II) complex residue.

As mentioned above, because the Stern–Volmer plot for RuQPIm-19 is nonlinear, the quenching reaction would proceed through not only dynamic quenching but also static quenching processes, or only a static process. We have reported that the MV^{2+} species undergo the π–π interaction with an imidazolyl residue on the RuQPIm-19 [15,18]. The binding of MV^{2+} species with the RuQPIm-19 having many imidazolyl residues should be multisteps, as expressed by Eqs. (6)–(9):

$$\text{RuQPIm-19} + MV^{2+} \overset{K_1}{\rightleftharpoons} (\text{RuQPIm-19} - MV^{2+}) \tag{6}$$

$$(\text{RuQPIm-19} - MV^{2+}) + MV^{2+} \overset{K_2}{\rightleftharpoons} (\text{RuQPIm-19} - 2MV^{2+}) \tag{7}$$

$$(\text{RuQPIm-19} - (n-1)MV^{2+}) + MV^{2+} \overset{K_n}{\rightleftharpoons} (\text{RuQPIm-19} - nMV^{2+}) \tag{8}$$

$$K_n = \frac{[\text{RuQPIm-19} - nMV^{2+}]}{[\text{RuQPIm-19} - (n-1)MV^{2+}][MV^{2+}]},$$
$$K_n = K_1/n \quad (n = 1, 2, 3, \ldots) \tag{9}$$

where RuQPIm-19–$n$$MV^{2+}$ represents the RuQPIm-19 to which n molecules of MV^{2+} are bound. The number of MV^{2+} molecules bound to the RuQPIm-19 obeys the Poisson distribution [23–25]. Here, we define the quenching by the MV^{2+} species undergoing π–π interaction as static quenching and propose two quenching models through both the dynamic and static quenching

Table 1
Kinetic parameters obtained from luminescence quenching data in the absence of L-tyrosine esters for these ruthenium (II) complexes

	τ_0 (ns)	Ksv (M^{-1})	kq_2 (M^{-1} s^{-1})	kq_1K_1
$Ru(bpy)_2(MeIm)_2^{2+}$	622	92.86	1.49×10^8	—
RuQPIm-19	628	—	—	1.33×10^8
RuQPIm-44	648	86.57	1.34×10^8	—

processes (model 1) and only the static quenching process (model 2). In model 1, the quenching reaction is divided into a dynamic process expressed by Eqs. (1)–(4) and a static process expressed as follows:

$$\text{RuQPIm-19} - n\text{MV}^{2+} \xrightarrow{h\nu'} {}^*\text{RuQPIm-19} - n\text{MV}^{2+} \quad (10)$$

$${}^*\text{RuQPIm-19} - n\text{MV}^{2+} \xrightarrow{k_e} \text{RuQPIm-19} - n\text{MV}^{2+} + h\nu \quad (11)$$

$${}^*\text{RuQPIm-19} - n\text{MV}^{2+} \xrightarrow{k_d} \text{RuQPIm-19} - n\text{MV}^{2+} \quad (12)$$

$${}^*\text{RuQPIm-19} - n\text{MV}^{2+} \xrightarrow{nkq_1} \text{RuQPIm-19} - n\text{MV}^{2+} \quad (13)$$

where kq_1 represents the first-order rate constant of quenching by the MV^{2+} species undergoing π–π interaction with the RuQPIm-19 and is proportional to the number of the interacted MV^{2+} molecules (n). Based on these equations [26,27], the Stern–Volmer plot for this model is represented by Eq. (14):

$$I_0/I = \frac{1 + Ksv[\text{MV}^{2+}]}{1 + Ksv[\text{MV}^{2+}][1 - \exp(-K_1[\text{MV}^{2+}])] - kq_1\tau_0K_1[\text{MV}^{2+}]} \quad (14)$$

In model 2, the dynamic quenching by the MV^{2+} species having no interaction in the bulk solution does not occur, whereas only a static quenching occurs. The reaction mechanism of this model is almost the same as that of model 1. By substituting $kq_2 = 0$ in Eq. (14), the Stern–Volmer plot for this model is expressed by Eq. (15).

$$I_0/I = \frac{1}{1 - kq_1\tau_0K_1[\text{MV}^{2+}]} \quad (15)$$

The observed Stern–Volmer plot fits the computed curve using Eqs. (14) and (15), indicating that the quenching reaction should obey either model 1 or model 2. Because the plot of I/I_0 against the concentration of MV^{2+} gives a straight line, however, the Stern–Volmer plot for this quenching would be given by Eq. (15) corresponding to model 2; namely, the dynamic quenching does not occur in this system. Our previous report showed the RuQPIm-19 shrank on addition of MV^{2+} in methanol [28]. Therefore, the shrinking of the RuQPIm-19 chain induced by π–π interaction of MV^{2+} species causes inhibition of the dynamic quenching process.

3.2. Quenching of RuQPIm-44 in the presence of L-tyrosine esters

For $Ru(bpy)_2(MeIm)_2^{2+}$, the Stern–Volmer plot does not change even on adding L-tyrosine esters, indicating that the L-tyrosine esters hardly affect the quenching reaction.

Fig. 4 shows the Stern–Volmer plots for quenching of RuQPIm-44 with MV^{2+} in the presence of L-tyrosine esters. The Stern–Volmer plots for all systems showed the downward deviating curves. It is known that the alkyl groups in the L-tyrosine esters (C_6Tyr, C_8Tyr and C_{12}Tyr) undergo van der Waals interaction with the alkyl side chains on the RuQPIm-44 and the enhancement of the quenching would be caused by mediation of the L-tyrosine esters [28]. For clarification of this quenching reaction, the quenching process mediated by the L-tyrosine esters, referred to as a mediated quenching process, would be important. Nonlinear Stern–Volmer plots suggest that the

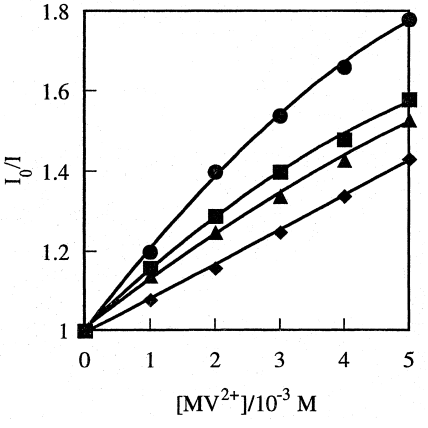

Fig. 4. Stern–Volmer plots for quenching of RuQPIm-44 with MV^{2+} in the absence (♦) and in the presence of L-tyrosine esters: C_6Tyr (●), C_8Tyr (■) and C_{12}Tyr (▲).

mediated quenching process does not proceed through a dynamic quenching process. Carraway et al. have proposed the Stern–Volmer plot for a two-site quenching model in which the quenching reaction takes place at two independent sites with different second-order quenching rate constants, as shown in Eq. (16) [29]:

$$I_0/I = \frac{1}{f_1/(1-kq_{21}\tau_0[Q]) + f_2/(1-kq_{22}\tau_0[Q])} \quad (f_1 + f_2 = 1) \tag{16}$$

where f_1 and f_2 represent the fractions of the sites having rate constants of k_{21} and k_{22}. The observed Stern–Volmer plots did not agree with the computed curve fitting according to Eq. (16). This result is evidence that the mediated quenching process does not proceed through the dynamic quenching process; namely, the mediated quenching process would proceed through a static quenching mechanism. Therefore, the quenching reactions for the L-tyrosine esters systems can be divided into two processes; a mediated quenching process and a non-mediated quenching one, which correspond to a static quenching process and a dynamic quenching process, respectively. For the dynamic quenching process, the quenching reaction proceeds as follows:

$$\text{RuQPIm-44(Tyr)}_m \xrightarrow{h\nu'} {}^*\text{RuQPIm-44(Tyr)}_m \tag{17}$$

$${}^*\text{RuQPIm-44(Tyr)}_m \xrightarrow{k_e} \text{RuQPIm-44(Tyr)}_m + h\nu \tag{18}$$

$${}^*\text{RuQPIm-44(Tyr)}_m \xrightarrow{k_d} \text{RuQPIm-44(Tyr)}_m \tag{19}$$

$${}^*\text{RuQPIm-44(Tyr)}_m + \text{MV}^{2+} \xrightarrow{kq_2} [\text{MV}^{2+}]\text{RuQPIm-44(Tyr)}_m + \text{MV}^{2+} \tag{20}$$

where RuQPIm-44(Tyr)_m represents the number of L-tyrosine esters undergoing van der Waals interaction with the RuQPIm-44. Furthermore, the static quenching process, corresponding to the mediated quenching process, can be expressed by Eqs. (21)–(28).

$$\text{RuQPIm-44(Tyr)}_m + \text{MV}^{2+} \overset{K_1}{\rightleftharpoons} \text{RuQPIm-44(Tyr)}_m - \text{MV}^{2+} \tag{21}$$

$$\text{RuQPIm-44(Tyr)}_m - \text{MV}^{2+} + \text{MV}^{2+} \overset{K_2}{\rightleftharpoons} \text{RuQPIm-44(Tyr)}_m - 2\text{MV}^{2+} \tag{22}$$

$$\text{RuQPIm-44(Tyr)}_m - (n-1)\text{MV}^{2+} + \text{MV}^{2+} \overset{K_n}{\rightleftharpoons} \text{RuQPIm-44(Tyr)}_m - n\text{MV}^{2+} \tag{23}$$

$$K_n = \frac{[\text{RuQPIm-44(Tyr)}_m - n\text{MV}^{2+}]}{[\text{RuQPIm-44(Tyr)}_m][\text{MV}^{2+}]} \quad K_n = K_1/n \quad (n = 1,2,3,\ldots) \tag{24}$$

$$\text{RuQPIm-44(Tyr)}_m - n\text{MV}^{2+} \xrightarrow{h\nu'} {}^*\text{RuQPIm-44(Tyr)}_m - n\text{MV}^{2+} \tag{25}$$

$${}^*\text{RuQPIm-44(Tyr)}_m - n\text{MV}^{2+} \xrightarrow{k_e} \text{RuQPIm-44(Tyr)}_m - n\text{MV}^{2+} + h\nu \tag{26}$$

$${}^*\text{RuQPIm-44(Tyr)}_m - n\text{MV}^{2+} \xrightarrow{k_d} \text{RuQPIm-44(Tyr)}_m - n\text{MV}^{2+} \tag{27}$$

$${}^*\text{RuQPIm-44(Tyr)}_m - n\text{MV}^{2+} \xrightarrow{nkq_1} \text{RuQPIm-44(Tyr)}_m - n\text{MV}^{2+} \tag{28}$$

Based on these equations, the Stern–Volmer plots for L-tyrosine esters systems are given by Eq. (14). The observed Stern–Volmer plots for these L-tyrosine esters systems agree well with the computed curve fitting according to the Eq. (14) ($R^2 = 0.999$). These kinetic parameters are summarized in Table 2.

Table 2
Kinetic parameters obtained from luminescence quenching data of RuQPIm-44 in the presence of L-tyrosine esters for these ruthenium (II) complexes

	τ_0 (ns)	Ksv (M^{-1})	kq_2 (M^{-1} s^{-1})	K_1 (M^{-1})	kq_1 (s^{-1})	kq_1K_1 (M^{-1} s^{-1})
RuQPIm-44						
C_6Tyr	648	109.38	1.69×10^8	310.88	5.57×10^5	1.73×10^8
C_8Tyr	648	87.30	1.35×10^8	432.39	3.39×10^5	1.47×10^8
C_{12}Tyr	648	76.85	1.19×10^8	625.37	2.28×10^5	1.43×10^8

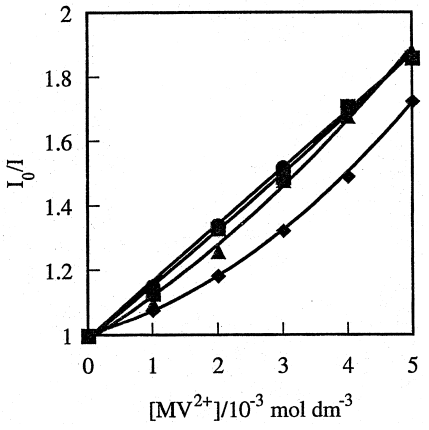

Fig. 5. Stern–Volmer plots for quenching of RuQPIm-19 with MV^{2+} in the absence (●) and in the presence of L-tyrosine esters: C_6Tyr (○), C_8Tyr (□) and C_{12}Tyr (△).

3.3. Quenching of RuQPIm-19 in the presence of L-tyrosine esters

Fig. 5 shows the Stern–Volmer plots for quenching of RuQPIm-19 with MV^{2+} in the absence and in the presence of the L-tyrosine esters. On addition of the L-tyrosine esters, the quenching reactions were enhanced, and the enhancement of the quenching slightly decreased with increasing length of the alkyl groups in the L-tyrosine esters. In these systems, the quenching reactions proceed the same as those in the RuQPIm-44 systems through a mediated quenching process and a non-mediated quenching one. As mentioned above, the non-mediated quenching process is expressed by Eqs. (6)–(13). The mediated process would proceed through a static quenching mechanism as mentioned in the RuQPIm-44 systems. Therefore, these quenching reactions proceed through two different static quenching processes. The mediated process proceeds as expressed by Eqs. (29)–(39):

$$\text{RuQPIm-19(Tyr)}_m + MV^{2+} \overset{K'_1}{\rightleftharpoons} \text{RuQPIm-19(Tyr)}_m - MV^{2+} \tag{29}$$

$$\text{RuQPIm-19(Tyr)}_m - MV^{2+} + MV^{2+} \overset{K'_2}{\rightleftharpoons} \text{RuQPIm-19(Tyr)}_m - 2MV^{2+} \tag{30}$$

$$\text{RuQPIm-19(Tyr)}_m - (m-1)MV^{2+} + MV^{2+} \overset{K'_m}{\rightleftharpoons} \text{RuQPIm-19(Tyr)}_m - nMV^{2+} \tag{31}$$

$$K'_m = \frac{[\text{RuQPIm-19(Tyr)}_m - nMV^{2+}]}{[\text{RuQPIm-19(Tyr)}_m][MV^{2+}]}, \quad K'_m = K_1/m \quad (m = 1,2,3,\ldots) \tag{32}$$

$$\text{RuQPIm-19(Tyr)}_m \xrightarrow{hv'} {}^*\text{RuQPIm-19(Tyr)}_m \tag{33}$$

$${}^*\text{RuQPIm-19(Tyr)}_m \xrightarrow{k_e} \text{RuQPIm-19(Tyr)}_m + hv \tag{34}$$

$${}^*\text{RuQPIm-19(Tyr)}_m \xrightarrow{k_d} \text{RuQPIm-19(Tyr)}_m \tag{35}$$

$${}^*\text{RuQPIm-19(Tyr)}_m + MV^{2+} \xrightarrow{kg'_2[MV^{2+}]} \text{RuQPIm-19(Tyr)}_m + MV^{2+} \tag{35}$$

$$\text{RuQPIm-19(Tyr)}_m - nMV^{2+} \xrightarrow{hv'} {}^*\text{RuQPIm-19(Tyr)}_m - nMV^{2+} \tag{36}$$

$${}^*\text{RuQPIm-19(Tyr)}_m - nMV^{2+} \xrightarrow{k_e} \text{RuQPIm-19(Tyr)}_m - nMV^{2+} + hv \tag{37}$$

$${}^*\text{RuQPIm-19(Tyr)}_m - nMV^{2+} \xrightarrow{k_d} \text{RuQPIm-19(Tyr)}_m - nMV^{2+} \tag{38}$$

$${}^*\text{RuQPIm-19(Tyr)}_m - nMV^{2+} \xrightarrow{kq'_1} \text{RuQPIm-19(Tyr)}_m - nMV^{2+} \tag{39}$$

where kq'_2 represents the second-order quenching rate constant and kq'_1 represents the first-order rate constant of quenching through the mediated quenching process. Furthermore, kq'_1 is different from kq_1 in Eq. (13), in which the rate of the mediated quenching process is independent of the MV^{2+} molecule bound. Based on Eqs. (6)–(13) and (29)–(39), Eq. (40) is represented:

$$I_0/I = \left[\frac{(1+kq'_2\tau_0[MV^{2+}])(1+kq'_1\tau_0)}{1+kq'_2\tau_0[MV^{2+}]+(kq'_1\tau_0-kq'_2\tau_0[MV^{2+}])\exp(-K'_1[MV^{2+}])}\right] \times \left[\frac{1+Ksv[MV^{2+}]}{1+Ksv[MV^{2+}][1-\exp(1-K_1[MV^{2+}])]-kq_1\tau_0K_1[MV^{2+}]}\right] \tag{40}$$

Table 3
Kinetic parameters obtained from luminescence quenching data of RuQPIm-19 in the presence of L-tyrosine esters for these ruthenium (II) complexes

	τ_0 (ns)	K_1' (M^{-1})	kq_1' (s^{-1})	$kq_1'K_1'$ (M^{-1} s^{-1})	kq_1K_1 (M^{-1} s^{-1})
RuQPIm-19					
C_6Tyr	628	444.33	5.14×10^5	2.28×10^8	1.04×10^8
C_8Tyr	628	380.11	4.68×10^5	1.78×10^8	1.08×10^8
C_{12}Tyr	628	378.60	3.99×10^5	1.51×10^8	1.18×10^8

By substituting $kq_2 = 0$ ($Ksv = 0$) and $kq_2' = 0$, a new Stern–Volmer plot for quenching reactions through two static quenching processes with different first-order rate constants is represented in Eq. (41).

$$I_0/I = \frac{(1 + kq_1'\tau_0)}{[1 + kq_1'\tau_0 \exp(-K_1'[MV^{2+}])][1 - kq_1\tau_0 K_1[MV^{2+}]]} \quad (41)$$

In fact, the observed Stern–Volmer plots agree with the computed curve using Eq. (41). The values of the kinetic parameters obtained from the computed curve fitting are summarized in Table 3.

4. Discussion

4.1. Quenching of RuQPIm-44

The quenching reaction proceeds as shown in Scheme 1.

The kq_2 values decrease with increasing length of the alkyl groups in the L-tyrosine esters. This is attributed to steric hindrance of the L-tyrosine esters, particularly C_{12}Tyr. As reported previously [28], these L-tyrosine esters undergo van der Waals interaction with the alkyl side chains on the RuQPIm-44, and the interaction increases with increasing length of the alkyl groups in the L-tyrosine esters. Probably, the C_{12}Tyr species having a long alkyl group cannot be completely incorporated into the polymer domain, and the C_{12}Tyr itself acts as steric hindrance to diffusion of the MV^{2+} species into the polymer domain, namely the dynamic quenching process. In contrast, the C_6Tyr and C_8Tyr can be completely incorporated into the polymer domain. Surprisingly, incorporation of the C_6Tyr species into the polymer domain brings about acceleration of the dynamic quenching process; the kq_2 value is larger than that of the $Ru(bpy)_2(MeIm)_2^{2+}$ system. The van der Waals interaction between the L-tyrosine esters and alkyl side chains on the RuQPIm-44 would restrict the fluidity of the alkyl side chains, leading to a decrease in the steric hindrance for the dynamic quenching process.

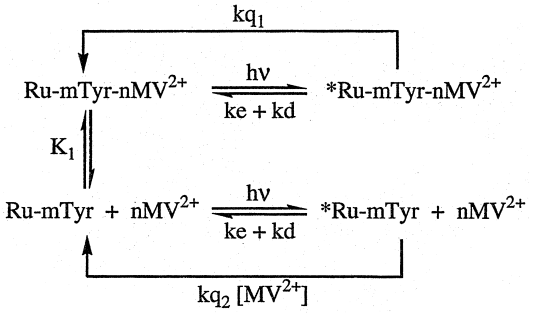

Scheme 1.

On the other hand, the kq_1 value, corresponding to the rate constant for the mediated quenching process, also decreases with increasing length of the alkyl groups in the L-tyrosine esters, while the K_1 value, corresponding to the equilibrium constant of complex formation between the MV^{2+} and the ruthenium (II) complex residue through the L-tyrosine ester, increases. That is to say, although the MV^{2+} species readily form the complex, the mediated quenching process is restricted. This result can be presumed as shown in Scheme 2. The complex formation would be affected by an electrostatic effect, electrostatic repulsion between the MV^{2+} species and polymer, and the increase in the alkyl groups in the L-tyrosine esters decreases the electrostatic repulsion: consequently, the K_1 value increases. In contrast, the kq_1 value would depend on the distance between the MV^{2+} and ruthenium (II) complex residue via L-tyrosine ester. Because the steric hindrance of alkyl groups in the L-tyrosine esters increases with increasing the length, the distance between reactive centers via the L-tyrosine esters increases, which leads to the decrease in the kq_1 value. When K_1 is regarded as pre-equilibrium constant for a bimolecular reaction as reported by Fouss [30], the second-order quenching constant for the mediated quenching process can be estimated by the product of K_1 and kq_1. The mediated quenching process is slightly faster than the dynamic quenching.

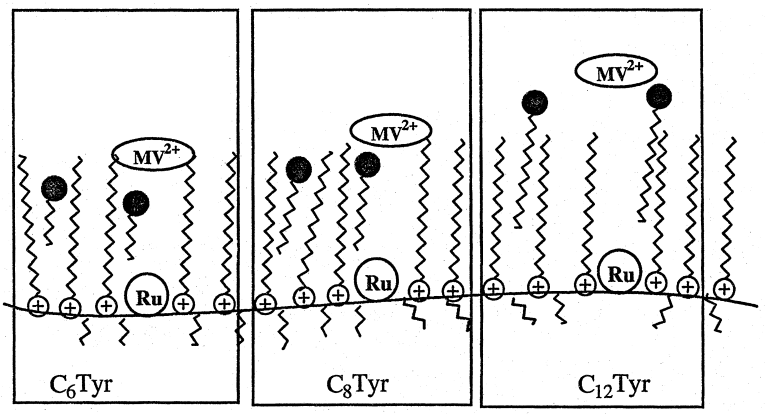

Scheme 2.

4.2. Quenching of RuQPIm-19

As mentioned above, the quenching reaction for RuQPIm-19 takes place with two different static quenching mechanisms, the mediated quenching process and non-mediated quenching one as described in Scheme 3.

We reported that the viscosity of the RuQPIm-19 is decreased by addition of the MV^{2+} and addition of L-tyrosine esters caused a further decrease in the viscosity in the order of $C_{12}Tyr > C_8Tyr > C_6Tyr$ [28]. These results led us to conclude that the volume of the polymer domain decreased. For the statically mediated quenching process, the kq'_1 and K'_1 values decrease with length of the alkyl groups in the L-tyrosine esters. Because the increase in the steric hindrance of the polymer chain, which is induced by the shrinking, restricts the complex formation (K'_1), kq'_1 also decreases, consequently leading to the restriction of the statically mediated quenching process (decrease in the $kq'_1K'_1$). Furthermore, kq'_1 for the $C_{12}Tyr$ system decreases in spite of a slight decrease in K'_1, indicating that $kq'_1K'_1$ value depends on kq'_1, but barely on K'_1. In contrast, the kq_1K_1 values for the statically non-mediated quenching process slightly increase with increasing length of the alkyl groups in the L-tyrosine esters. This result agrees with the order of an increase in the volume of the polymer domain. Because the increase in the volume decreases the steric hindrance for the complex formation (K_1), the K_1 value increases, and the kq_1K_1 values increase. Compared with the value in the absence of L-tyrosine ester, however, the kq_1K_1 values are small. This result can also be explained based on the same reason mentioned above. On the other hand, the $kq'_1K'_1$ value is larger than the kq_1K_1, indicating that the mediated quenching process is faster than the non-mediated quenching process. These results suggest that the MV^{2+} species undergoing π–π interaction with the polymer backbone participate in the statically mediated quenching process, but not the MV^{2+} species having no interaction with the polymer in the bulk solution, which is supported by the fact that the K'_1 value decreases with increasing volume of the polymer domain. The complex formation between the MV^{2+} species in the bulk solution and ruthenium (II) complex residue through the L-tyrosine ester barely depends on the volume of the polymer domain. If it depended on domain volume,

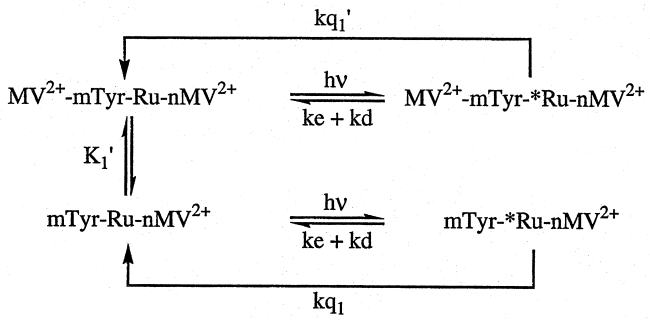

Scheme 3.

the K'_1 value would increase with increasing the domain volume because the steric hindrance decreases. Compared with the RuQPIm-44 systems, the quenching rate constants for the mediated quenching process, $K'_1kq'_1$ for RuQPIm-19 and K_1kq_1 for RuQPIm-44, are large because the electrostatic repulsion is smaller than that of RuQPIm-44.

5. Conclusions

We kinetically analyzed the quenching of RuQPIm-19 and RuQPIm-44 with MV^{2+} and revealed the effects of the L-tyrosine esters on the quenching reactions. In the absence of L-tyrosine esters, the Stern–Volmer plots show a straight line for RuQPIm-44 and an upward deviating curve for RuQPIm-19, the quenching reactions proceed through only a dynamic quenching process for RuQPIm-44 and through only a static quenching process for RuQPIm-19. These reaction mechanisms are varied by addition of the L-tyrosine esters. For RuQPIm-44, the Stern–Volmer plots show the downward deviating curves. The computed curve fittings to the observed Stern–Volmer plots indicate that the quenching reactions take place through both the dynamic quenching and static quenching processes: consequently, the mediated quenching process proceeds statically. In contrast, the quenching reactions for the RuQPIm-19 systems proceed through two different static quenching processes. A new Stern–Volmer plot is proposed as expressed by Eq. (41), and the kinetic parameters can be estimated. These kinetic parameters depend significantly on the length of the alkyl groups in the L-tyrosine esters.

Acknowledgements

We would like to thank Professor M. Kaneko (Department of Chemistry, Ibaraki University) and Professor M. Yagi (Faculty of Education, Niigata University) for the luminescence lifetime measurements.

References

[1] Palmer G, editor. Long range electron transfer in biology. Structure and bonding, vol. 75. Berlin: Springer, 1991.
[2] Electron transfer in inorganic, organic and biological systems. In: Bolton JR, Mataga N, MacLendon G, editors. ACS Advances in Chemistry Series No. 228. Washington, DC: American Chemical Society, 1991.
[3] Fox MA, Chanon M, editors. Photoinduced Electron Transfer. Amsterdam: Elsevier, 1988.
[4] Axup AW, Albin M, Mayo SL, Crutchley RJ, Gray HB. J Am Chem Soc 1988;110:435.
[5] Bowler BE, Meade TJ, Mayo SL, Richards JH, Gray HB. J Am Chem Soc 1989;111:8757.
[6] Beratan DN, Onuchic JN, Betts JN, Bowler BE, Gray HB. J Am Chem Soc 1990;112:7915.
[7] Farver O, Pecht I. J Am Chem Soc 1992;114:5764.
[8] Siddarth P, Marcus RA. J Phys Chem 1993;97:2400.
[9] Barry BA. Photochem Photobiol 1993;57:179.
[10] Kaneko M, Moriyoshi J, Yamada A. Nature 1980;285:468.
[11] Milosavljevic BH, Thomas JK. J Phys Chem 1985;89:1830.
[12] Colon J, Yang C-Y, Clearfield A, Martin CR. J Phys Chem 1990;94:874.
[13] Nagai K, Tsukamoto J, Takamiya N, Kaneko M. J Phys Chem 1995;99:6648.
[14] Yagi M, Kinoshita K, Kaneko M. J Phys Chem B 1997;101:3957.
[15] Suzuki M, Mori Y, Kimura M, Hanabusa K, Shirai H. J Chem Soc Faraday Trans 1996;92:3599.
[16] Suzuki M. Kobayashi S. Kimura M. Hanabusa K. Shirai H. Chem Commun 1997;227.
[17] Suzuki M, Kimura M, Hanabusa K, Shirai H. Macromol Chem Phys 1998;199:945.
[18] Suzuki M, Yokoyama N, Mori Y, Kimura M, Hanabusa K, Shirai H. Macromol Chem Phys 1997;198:957.
[19] Geraty SM, Vos JG. J Chem Soc Dalton Trans 1987;3073:.
[20] Kohn J, Langer R. J Am Chem Soc 1987;109:817.
[21] Forster RJ, Vos JG. Macromolecules 1990;23:4372.
[22] Stern VO, Volmer M. Z Phys 1919;20:183.
[23] Morishima Y, Itoh Y, Nozakura S. Chem Phys Lett 1982;91:258.
[24] Yekta A, Aikawa M, Turro TJ. Chem Phys Lett 1979;63:543.
[25] Infelta PP. Chem Phys Lett 1979;61:88.
[26] Kaneko M, Hou X-H, Yamada A. Bull Chem Soc Jpn 1987;60:2523.
[27] Nagai K, Takamiya N, Kaneko M. Macromol Chem Phys 1996;197:2983.
[28] Suzuki M, Sano M, Kimura M, Hanabusa K, Shirai H. Eur Polym J 1999;35:221.
[29] Carraway ER, Demas JN, DeGraff BA, Bacon JR. Anal Chem 1991;63:337.
[30] Fouss RM. J Am Chem Soc 1958;80:5059.